

Optimized geometries for optical lattices

A,¹ B,¹ and C¹

¹Department of Physics, Harvard University, Cambridge, Massachusetts 02138, USA

This is the abstract.

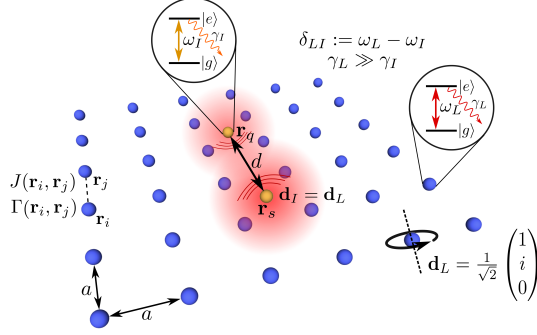


Figure 1. •

I. INTRODUCTION

II. MODEL

[arb. geometry, Green's Tensor, Couplings, Polarizations -> Distance dependence, Hamiltonian, Self-energy, Ref. to Taylor's work]

We consider two-dimensional sub-wavelength lattices of quantum emitters which interact via resonant dipole-dipole interactions. The emitters are assumed to be two-level stems with a ground state $|g\rangle$ and an excited state $|e\rangle$ with a transition frequency $\omega_L = ck_L$, such that $k_L = 2\pi/\lambda_L$ denotes the related wavenumber with the resonance wavelength λ_L . Pairwise resonant dipole-dipole interactions among emitters result in collective couplings J_{ij} and collective decay rates Γ_{ij} between emitters i and j at positions \mathbf{r}_i and \mathbf{r}_j , given by

$$J_{ij} = -\frac{3\pi\sqrt{\gamma_i\gamma_j}}{\omega_L} \hat{\mathbf{d}}_i^\dagger \cdot \mathbf{Re}[\mathbf{G}(\mathbf{r}_{ij}, \omega_L)] \cdot \hat{\mathbf{d}}_j \quad (1a)$$

$$\Gamma_{ij} = \frac{6\pi\sqrt{\gamma_i\gamma_j}}{\omega_L} \hat{\mathbf{d}}_i^\dagger \cdot \mathbf{Im}[\mathbf{G}(\mathbf{r}_{ij}, \omega_L)] \cdot \hat{\mathbf{d}}_j \quad (1b)$$

where γ_i and γ_j are the decay rates of the individual dipoles i and j , and $\mathbf{r}_{ij} = \mathbf{r}_i - \mathbf{r}_j$ is the displacement vector. $\mathbf{G}(\mathbf{r}_{ij}, \omega_L)$ is the Green's tensor, defined as

$$G_{\alpha\beta}(\mathbf{r}, \omega) = \frac{e^{i\omega r}}{4\pi r} \left[\left(1 + \frac{i}{\omega r} - \frac{1}{\omega^2 r^2} \right) \delta_{\alpha\beta} - \left(1 + \frac{3i}{\omega r} - \frac{3}{\omega^2 r^2} \right) \frac{r_\alpha r_\beta}{r^2} \right] - \frac{\delta(\mathbf{r})}{3\omega^2} \delta_{\alpha\beta} \quad (2)$$

\mathbf{d}_i and \mathbf{d}_j are the dipole polarizations, which are set to be uniformly circular, so that $\hat{\mathbf{d}}_L = \hat{\mathbf{d}}_I = \frac{1}{\sqrt{2}} \begin{pmatrix} 1 & i & 0 \end{pmatrix}^T$

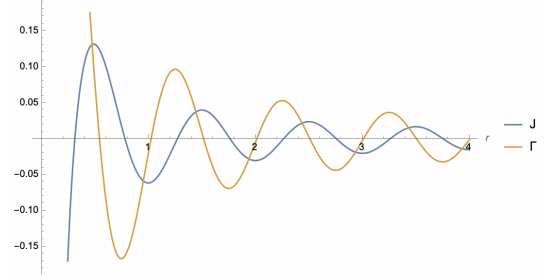


Figure 2. •

where $\hat{\mathbf{d}}_L$ is the polarization of the lattice dipoles, and $\hat{\mathbf{d}}_I$ is the polarization of any impurities. This polarization ensures that the dynamics of the system depend purely on the relative distances r_{ij} between pairs of dipoles, independent of their relative orientations. As a result, J_{ij} and Γ_{ij} can be written as

$$J_{ij} = -\frac{3}{8\omega_L r_{ij}} \left(\cos(\omega_L r_{ij}) + \frac{\sin(\omega_L r_{ij})}{\omega_L r_{ij}} + \frac{\cos(\omega_L r_{ij})}{(\omega_L r_{ij})^2} \right) \quad (3a)$$

$$\Gamma_{ij} = \frac{3}{4\omega_L r_{ij}} \left(\sin(\omega_L r_{ij}) - \frac{\cos(\omega_L r_{ij})}{\omega_L r_{ij}} + \frac{\sin(\omega_L r_{ij})}{(\omega_L r_{ij})^2} \right) \quad (3b)$$

In this way, collective couplings (Fig. ??) and collective decay rates (Fig. ??) depend purely on the relative distances r_{ij} between pairs of dipoles, independent of their relative orientations. Into this lattice, we place one or two lattice impurities with transition frequency $\omega_I \approx \omega_L$. The overall Hamiltonian is $H = H_L + H_{LI} + H_I$, where H_L is the Hamiltonian of the lattice, H_{LI} is the Hamiltonian for the interaction between the lattice and any impurities, and H_I is for the interactions involving just impurities. These Hamiltonians are defined such that

$$H_L = \sum_i^{N_L} \left(\omega_L - \frac{i}{2}\gamma_L \right) \sigma_i^\dagger \sigma_i + \sum_{i,j \neq i}^{N_L} \left(J_{ij} - \frac{i}{2}\Gamma_{ij} \right) \sigma_i^\dagger \sigma_j \quad (4a)$$

$$H_{LI} = \sum_i^{N_L} \sum_j^{N_I} \left[\left(J_{ij} - \frac{i}{2}\Gamma_{ij} \right) \sigma_i^\dagger s_j + \left(J_{ji} - \frac{i}{2}\Gamma_{ji} \right) s_j^\dagger \sigma_i \right] \quad (4b)$$

$$H_I = \sum_j^{N_I} \left(\omega_I - \frac{i}{2}\gamma_I \right) s_j^\dagger s_j + \sum_{i,j \neq i}^{N_I} \left(J_{ij} - \frac{i}{2}\Gamma_{ij} \right) s_i^\dagger s_j \quad (4c)$$

where N_L is the number of lattice atoms, σ_i is the lowering operator for lattice atom i , N_I is the number of impurities, and s_j is the lowering operator for impurity j .

III. SINGLE IMPURITY CASE

[Define lattices, define distances related to lattices, Γ_{eff} , constant area]

The generic form of the Hamiltonian for a given lattice of N atoms along with a single impurity is

$$H = \begin{pmatrix} & & C_{LI} \\ & H_L & \vdots \\ C_{IL} & \cdots & C_{IL} & H_I \end{pmatrix} \quad (5)$$

where H_L represents the $N \times N$ matrix of terms for the lattice's own Hamiltonian, H_I is the lattice, and C_{IL} along with C_{LI} represent the coupling terms between the lattice atoms and the impurity.

Define the wavefunction such that $\psi = (b_1 \ : \ b_N \ : \ c)^T$, and assume that the lattice occupies a steady state, so that the Schrödinger equation is

$$i\hbar \begin{pmatrix} 0 \\ \vdots \\ 0 \\ \dot{c} \end{pmatrix} = \begin{pmatrix} & & C_{LI} \\ & H_L & \vdots \\ C_{IL} & \cdots & C_{IL} & H_I \end{pmatrix} \begin{pmatrix} b_1 \\ \vdots \\ b_N \\ c \end{pmatrix} \quad (6)$$

This can be solved to get

$$\begin{pmatrix} b_1 \\ \vdots \\ b_N \end{pmatrix} = -H_L^{-1} C_{LI} c \quad (7)$$

Putting this back into the Schrödinger equation produces

$$\dot{c} = -i(H_I - C_{LI}^T H_L^{-1} C_{LI})c \quad (8)$$

Recognizing that $H_I - C_{LI}^T (H_L^{-1}) C_{LI} = \Sigma_I - i\frac{\gamma_I}{2}$, we can calculate the impurity's self-energy Σ_I to be

$$\Sigma_I = H_I - C_{LI}^T (H_L^{-1}) C_{LI} + i\frac{\gamma_I}{2} \quad (9)$$

The effective decay rate Γ_{eff} for an impurity in the lattice is related to this self-energy according to

$$\Gamma_{\text{eff}} = \gamma_I - 2 \text{Im}[\Sigma_I] \quad (10)$$

Equipped with these mathematical tools, we consider the full range of non-centered Bravais lattices, for both interstitial and substitutional impurity positions, as illustrated in Fig. 3. In order to reasonably compare lattices of differing geometries, we ensure, whenever possible, that all plaquettes possess the same area throughout all possible transformations.

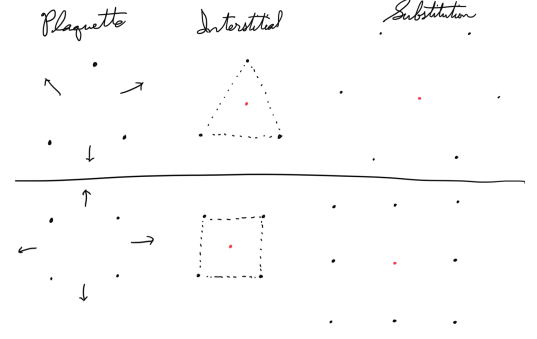


Figure 3. • [This needs to be remade so that a top line illustrates all four Bravais lattices, and a line below that illustrates the difference between the substitutional and interstitial cases. A brute force version of the bottom lines would just be to show the full lattices for each case, so that the figure later on of the substitutional triangular case could be incorporated as one amongst the eight full lattices depicted on the bottom two lines. It would at least be thorough.]

A. Interstitial

Consider a finite square lattice, with an inter-atomic spacing of $a = 0.2$, defined as a function of the lattice's resonant wavelength. Compare this to the other Bravais lattices, namely a triangular lattice, and monoclinic lattice defined over θ from $\pi/2$ to 0, and a rectangular lattice with a scaling factor μ such that the horizontal sidelength of its rectangular plaquette is μa . [Which variable do we want for scaling? Does μ work?.] To ensure that the plaquettes of all of these lattices have the same area, we set the sidelength of the triangular plaquettes to $\frac{2}{3^{1/4}}a$, the height of monoclinic lattices to a for all θ , and the height of the rectangular lattices to a/μ .

For an interstitial impurity, the position of the impurity in the plaquette along with its detuning relative the lattice's resonant frequency determine its decay properties. Detuning is defined as $\delta_{LI} = \omega_I - \omega_L$. For a given impurity position, δ_{LI} can be chosen to give optimal Γ_{eff} , by minimizing along a curve such as Fig. 5. By conducting this optimization for all positions within a plaquette, a map of the optimal impurity placement can be constructed. The results of this are depicted in Fig. 4. See the appendix for the values of δ_{LI} corresponding to these impurity positions.

In all cases, geometric symmetries determines where the points of minimal Γ_{eff} lie. The paths of minimal Γ_{eff} follow the geometry of a Voronoi diagram constructed around the lattice atoms. The vertices where edges of this Voronoi partition meet are then the points of minimal Γ_{eff} , which are often the global minima as well. The number of edges that coincide at any one point roughly correlates to how low the effective decay rate will be compared to other such points. For instance, the center of

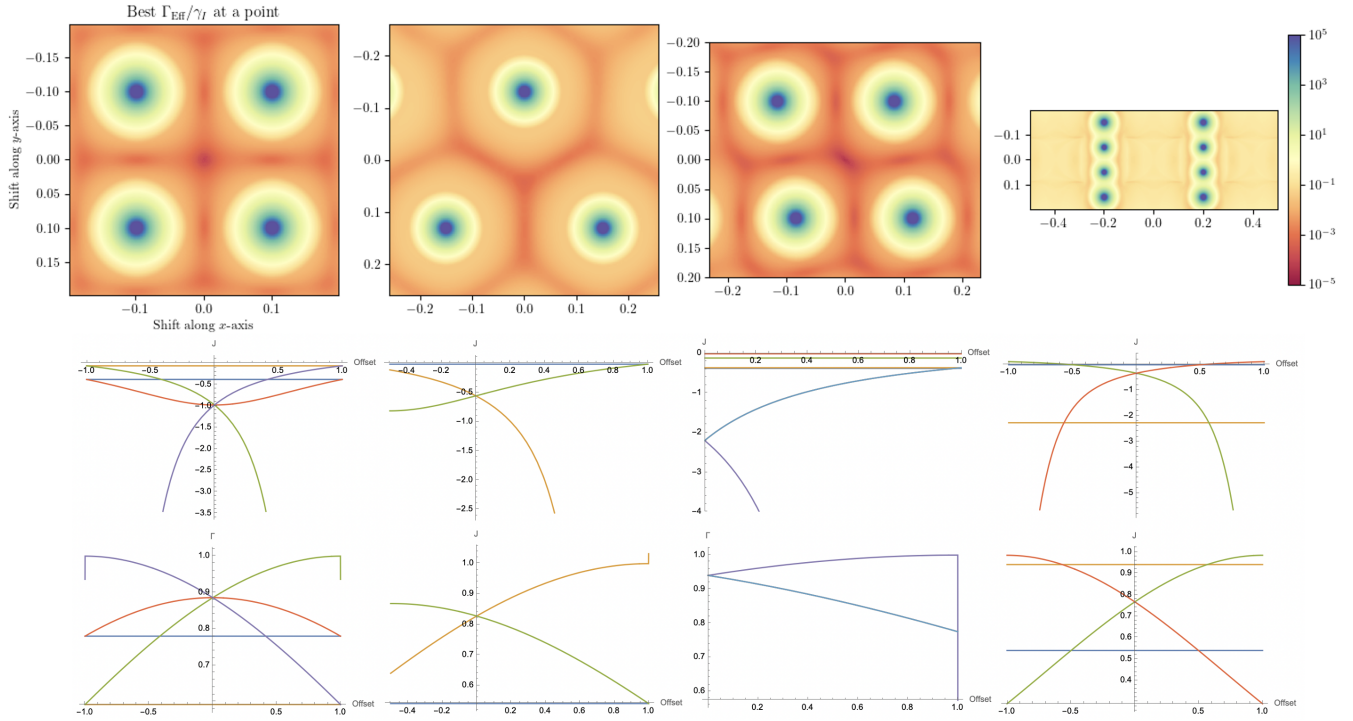


Figure 4. •[To do: 1) Change monoclinic plaquette to something more like $\theta = 0.4$. 2) Change rectangular scaling to something more like 1.5 or 1.3. 4) Update the Mathematica lineplots to match this, because even now, they were made for the wrong θ and scaling. 3) Draw line paths across all the plaquettes, illustrating which paths the plots are graphed over]

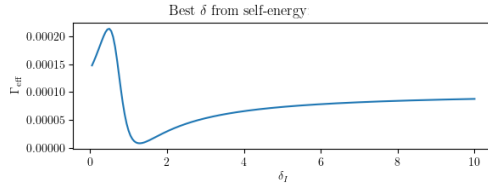


Figure 5. •

the square plaquette, where four edges coincide, has an optimal Γ_{eff} (7.58×10^{-5} [units]) that is approximately an order of magnitude less than the optimal Γ_{eff} at the center of the triangular plaquette (6.75×10^{-4} [units]), where only three edges coincide. Note that this Voronoi structure does not always result in the center of the plaquette becoming the optimal position for an impurity, as demonstrated by the monoclinic case. The optimal positions are just off the center, on the line of symmetry along the long axis of the plaquette, at a pair of points where three Voronoi edges meet. As θ approaches $\frac{\pi}{2}$, these two points merge into one, at the center of a square plaquette.

[This suggests that we should try a hexagonal plaquette of the same area, and that we will get an even better result from that!]

Not a Bravais lattice, but surely still worth a try.]

The role that symmetry plays in creating these Voronoi geometries is clear once the couplings J_{ij} and Γ_{ij} between pairs of particles are plotted over a path through the plaquette space. At points of geometric symmetry, such as the centers of plaquettes, the values of these couplings coincide. In general, the more that couplings match, the lower the Γ_{eff} for an impurity placed at the point. In this way, lattices with higher degrees of symmetry (i.e. the square and triangular lattices), and with higher numbers of atoms in a single plaquette (i.e. any Bravais lattice other than the triangular lattice) possess impurity positions with the smallest Γ_{eff} . The fact that the square lattice possesses both of these properties helps to explain why it stands out amongst the various Bravais lattices as the optimal choice.

[Look at the "unscaled example.png," and see how it shows that not must the nearest neighbors, but the second-nearest neighbors also matter to ensuring a small Γ_{eff} at the center. Then make this point in the paper, that the collective modes are not just governed by nearest neighbors.]

B. Substitutional

Now, considering substituting a lattice atom for an impurity, so that, in effect, the impurity takes up a vacancy in the lattice. In general, the impurity positions available when an impurity is substituted for a lattice atom result in Γ_{eff} that are sub-optimal compared to an interstitial impurity placement (Fig. 6). The best positions for a substitution are also almost always off-center, as an impurity substitution in the exact position of where a lattice atom should be tends to put the Γ_{eff} of the impurity in the region of a local maximum. Offsetting the impurity so that it lies approximately midway between a lattice atom and the vacancy left by the lattice atom that is replaced returns it to a local maximum.

[Can this argument be made more clear if we add high-contrast version of the hexagonal and rectangular plots?]

The symmetry of the lattice is already broken by substituting an offset impurity for a lattice atom, and so symmetry does not play as great a role in determining the optimal impurity position compared to the interstitial case. If there is any role for symmetry, it is between the lattice atoms and the vacancy made by the substitution, so that the impurity receives the best Γ_{eff} when it sits between these points.

[There is surely more to say. For instance, why is the hexagonal case so much worse than the monoclinic case?]

For all Bravais lattices, across all monoclinic angles and rectangular scalings, the optimal Γ_{eff} for a substitutional impurity placement is always greater than the optimal Γ_{eff} for an interstitial impurity. As a result, to optimize for the longest lifetime of the impurity's excited state, an interstitial placement is best for any Bravais lattice.

[Demonstrate this with a figure that shows the optimal Γ_{eff} for all theta and scalings. My current plot is inadequate for this, especially, since it keeps the impurity in the center of the plaquette when the best position for a monoclinic lattice is off-center.]

C. Varying scaling factors

IV. TWO IMPURITY CASE

[Q-factor, analyze different lattices -> discuss the most important figures, constant distance]

Γ_{eff} for a lattice with two impurities is calculated in a manner analogous to the single-impurity case, starting with the Schrödinger equation for the two-impurity Hamiltonian, for which

$$i\hbar \begin{pmatrix} 0 \\ \vdots \\ 0 \\ \dot{c} \\ \dot{d} \end{pmatrix} = \begin{pmatrix} & & C_{L1} & C_{L2} \\ & H_L & \vdots & \vdots \\ C_{1L} & \cdots & C_{1L} & H_1 & C_{12} \\ C_{2L} & \cdots & C_{2L} & C_{21} & H_2 \end{pmatrix} \begin{pmatrix} b_1 \\ \vdots \\ b_N \\ c \\ d \end{pmatrix} \quad (11)$$

In this way,

$$b = -(H_L)^{-1}(C_{L1}c + C_{L2}d) \quad (12)$$

Putting this result back into the Schrödinger equation gives

$$\dot{c} = -i [H_1 - C_{1L}^T (H_L)^{-1} C_{L1}] c - i [C_{12} - C_{1L}^T (H_L)^{-1} C_{L2}] d \quad (13a)$$

$$\dot{d} = -i [C_{21} - C_{2L}^T (H_L)^{-1} C_{L1}] c - i [H_2 - C_{2L}^T (H_L)^{-1} C_{L2}] d \quad (13b)$$

Let $\dot{c} = -i[\Sigma_1 - \frac{i\gamma_1}{2}]c - i\kappa_1 d$ and $\dot{d} = -i[\Sigma_2 - \frac{i\gamma_2}{2}]d - i\kappa_2 c$, where κ_1 and κ_2 are "effective couplings." Solving for these and the self-energies results in

$$\Sigma_1 = H_1 - C_{1L}^T (H_L)^{-1} C_{L1} + \frac{i\gamma_1}{2} \quad (14a)$$

$$\Sigma_2 = H_2 - C_{2L}^T (H_L)^{-1} C_{L2} + \frac{i\gamma_2}{2} \quad (14b)$$

$$\kappa_1 = C_{12} - C_{1L}^T (H_L)^{-1} C_{L2} \quad (14c)$$

$$\kappa_2 = C_{21} - C_{2L}^T (H_L)^{-1} C_{L1} \quad (14d)$$

The impurities' effective decay rates are determined by $\Gamma_{\text{eff},i} = \gamma_i - 2 \text{Im}[\Sigma_i]$, where i stands for either the first or second impurity. Likewise, we define the Q-factor as a function of the effective decay rate and the effective coupling, so that $Q_i = \frac{\text{Re}[\kappa_i]}{\Gamma_{\text{eff},i}}$ for each of the two impurities. Because the first and second impurities occupy symmetric positions in the lattice, we find that $\Gamma_{\text{eff},1} = \Gamma_{\text{eff},2}$ and $Q_1 = Q_2$. We thus consolidate these variables, so that we may speak of the impurities' effective decay rate Γ_{eff} and overall quality factor Q .

A. Monoclinic lattice

B. Rectangular lattice

V. CONCLUSIONS AND OUTLOOK

These are the Conclusions.

Acknowledgments. We would like to thank [add people]. This work was supported by [add funding sources]

The numerical simulations were performed with the open-source framework `QuantumOptics.jl` [1].

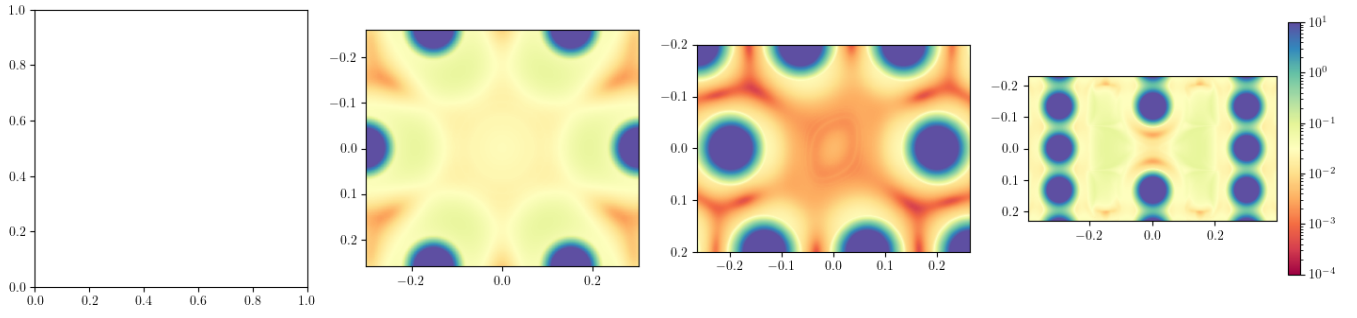


Figure 6. •

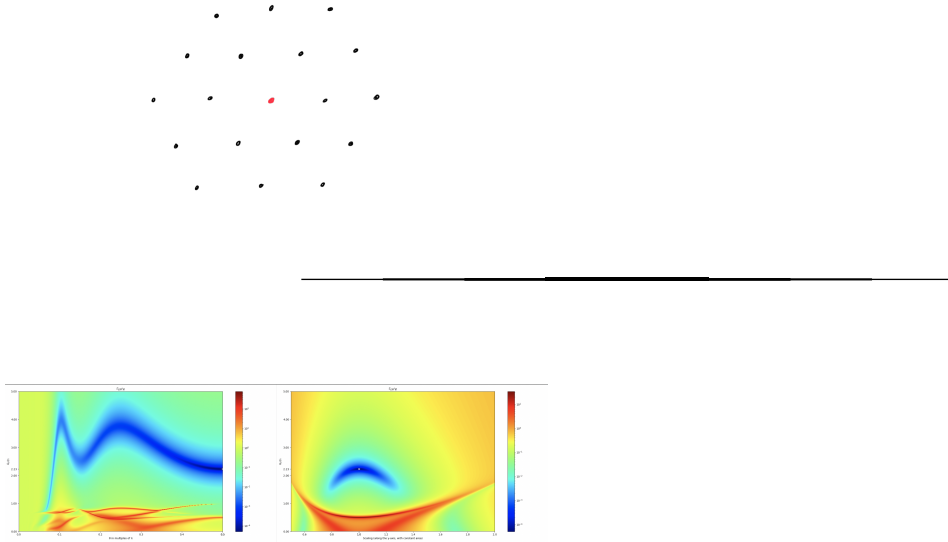


Figure 7. •[Reproduce this plot with the impurity kept at the Voronoi vertices and not at the center. Use the analytical definition of the Voronoi vertices, so that you don't have to optimize for every theta.]

[1] S. Krämer, D. Plankensteiner, L. Ostermann, and H. Ritsch, QuantumOptics.jl: A Julia framework for sim-

ulating open quantum systems, *Computer Physics Communications* **227**, 109 (2018).

Figure 8. •[Make a bar plot of the minimal Gamma eff for all eight of the cases considered in this section. Use this to prove that the interstitial case is always better than the substitutional. Also, on the plaquette plot figures, mark where these minima are with an arrow.]